HIGH-THROUGHPUT TRANSFER IMPRINTING

FOR ORGANIC SEMICONDUCTORS

A Thesis

by

GIHOON CHOO

Submitted to the Office of Graduate Studies of
Texas A&M University
in partial fulfillment of the requirements for the degree of

MASTER OF SCIENCE

Chair of Committee,	Xing Cheng
Committee Members,	Haiyan Wang
	Jim Ji
	Choongho Yu
Head of Department,	Chanan Singh

August 2013

Major Subject: Electrical Engineering

Copyright 2013 Gihoon Choo

ABSTRACT

Development of nanoimprint lithography(NIL) has enabled high-throughput and high-resolution patterning over the optical limitation. In recent years, thermal nanoimprint has been used to directly pattern functional materials such as organic semiconductors because heat and pressure used in thermal nanoimprint do not damage functional materials. However, issues such as residual layer removal and mold contamination still limit the application of nanoimprint for organic semiconductor patterning.

In this work, nanoimprint-based transfer imprinting of organic semiconductor is studied. In the same time the suggested technique is simulated with COMSOL multi-physics simulator to understand its mechanism. This transfer printing technique utilize thermal nanoimprint scheme to enable residual-layer-free patterning of organic semiconductors without mold contamination. The transfer imprinting technique is amenable to roll-to-roll process for high-throughput patterning of organic semiconductors for low-cost organic electronic applications.

ACKNOWLEDGEMENTS

First of all I would like to thank my family members who have supported me consistently throughout all my life. It is my luck having a family who are always there for me.

I also would like to thank my committee chair, Dr. Xing Cheng, and my committee members, Dr. Haiyan Wang, Dr. Jim Ji, Dr. Choongho Yu, for their guidance and support throughout the course of this research.

My research group was also very helpful during these past years. I would like to especially thank Wonsuk Lee, Youwei Jiang, Yi-chen Lo, Yunbum Jung, Bingquing Luo and Ning Xia. All of them were friendly and helpful in office and in the lab.

Thanks to my friends and colleagues, A&M Korean Presbyterian Church members, and Akoz basketball team members who have energized and vitalized my life in College Station.

For the last, thanks to the department faculty and staff for making my time at Texas A&M University a great experience.

TABLE OF CONTENTS

	Page
ABSTRACT	ii
ACKNOWLEDGEMENTS	iii
TABLE OF CONTENTS	iv
LIST OF FIGURES	v
LIST OF TABLES	vii
CHAPTER I INTRODUCTION:	1
CHAPTER II PROBLEM STATEMENT	17
CHAPTER III NANOIMPRINT BASED TRANSFER PRINTING	23
3.1 Process description	23
3.2 Experimental details	24
3.3 Materials	27
3.4 Experimental results	30
CHAPTER IV SIMULATION AND MODELING	34
4.1 Geometric modeling	34
4.2 Process physics modeling	34
4.3 Simulation results	37
CHAPTER V DISCUSSION	41
CHAPTER VI CONCLUSION	44
REFERENCES	46

LIST OF FIGURES

Page

Figure 1 Major steps in the photolithography process... 3

Figure 2 Concept of phase shift mask (PSM) technique 5

Figure 3 Lithography exposure tool potential solutions (ITRS 2009).................... 6

Figure 4 Major steps of thermal NIL process 9

Figure 5 Major steps of UV nanoimprint process 11

Figure 6 Two methods of roller nanoimprint lithography 13

Figure 7 Steps of LADI process 15

Figure 8 Concept of roller imprinting based on focus infrared heating 16

Figure 9 The process of organic vapor phase deposition(OVPD)
and thermal printing 19

Figure 10 The schematic of transfer printing 21

Figure 11 Steps of soft stamp polymer transfer printing 22

Figure 12 A schematic of the nanoimprint-based transfer printing 24

Figure 13 PDMS surface modification 28

Figure 14 Chemical structure of Cyclotene 29

Figure 15 Microscope images of transferred P3HT patterns 31

Figure 16 Transferred pattern width with different PDMS thickness 32

Figure 17 Images of 50um P3HT line patterns.. 33

Figure 18 Geometric modeling of the nanoimprint-based
transfer imprinting process.. 35

Figure 19 2-D total displacement results 38

Figure 20 1-D and 2-D pressure distribution graph at the substrate surface 40

Figure 21 Simulation results correspond to the experimental results 41

Figure 22 Process analysis graphs. 45

LIST OF TABLES

Page

Table 1 Quantitative experiment variables & ranges 27

Table 2 Measured adhesion layer thickness on silicon substrate with different dilute ratio... 30

Table 3 Equations of Comsol solid structure mechanics model 36

Table 4 PDMS material properties... 36

Table 5 Critical pressure extraction.. 42

CHAPTER I

INTRODUCTION

Semiconductor industry has grown very fast, since semiconductor is introduced. The development of electronic device fabrication process, especially development of lithography technique which transfers a desired graphic pattern on to the substrate, made possible this fast advancement of semiconductor industry. Many kinds of lithography processes have been introduced by many scientists to improve feature resolution, such as extreme ultra-violet (EUV) lithography, electron beam (e-beam) lithography, x-ray lithography, ion beam lithography and nanoimprint lithography (NIL). Lithography systems for manufacturing should satisfy some basic requirement: critical dimension control, capability of pattern overlay, high process yield, low defect density, low cost tooling and fabrication. Currently photolithography technique has been mainly used by semiconductor industry for mass production. Also photolithography technique has been used and satisfied the demands for higher resolution features to keep up with Moore's law for decades. However optical lithography technique is now facing limitation to follow higher resolution demands of industry due to its wavelength limitation.[1, 2]

The major steps of the photolithography process are illustrated in Figure1. The first step is coating UV sensitive photoresist on the substrate. A spin-coating method is widely used for the step. After coating, a short bake at about 90C is applied to remove solution from the resist. The second step is exposing the photoresist with UV light source through an optical system and a photo-mask as illustrated in Figure 1(b). An exposed photoresist shows different reaction depends on its resist types. Positive

photoresists contain stabilizer which slows down the dissolution rate of the resist when placed in the developer. When positive resist exposed to the UV light, stabilizer is destroyed that exposed areas dissolve easily. While resists, at the unexposed area remain hard to wash away in the developer due to undestroyed stabilizer. In negative photoresist, polymers cross-link at the UV light exposed areas become hard to wash away with developer. On the other hand, unexposed areas remain easy to wash away. Results of the exposure showed in the Figure 1(c). The following step is etching the silicon oxide layer with buffered hydrofluoric acid (HF). Due to the photoresist, silicon oxide layer will etched out selectively. The last step is resist strip, which removes the remaining photoresist by using chemical solution. After all these processes, patterns on the photo mask are transferred on to the substrate as illustrated in Figure 1(d). [1, 2]

Photolithography process is limited by the diffraction of the light. The approximated minimum feature size of projection lithography system follows this equation:

$$\text{CD(critical dimesion)} = k1 \cdot \frac{\lambda}{NA} \tag{1.1}$$

Here λ is the wavelength of the light source used in photolithography, NA is the numerical aperture of the optical lens system and k_1 is a coefficient that depends on the processing factors on the range of 0.25 to 0.8 (<0.1). According to the formula (1.1), the minimum feature size shrinks as wavelength of the light source decreases and as NA increases. However, using shorter wavelength source is limited due to several factors.

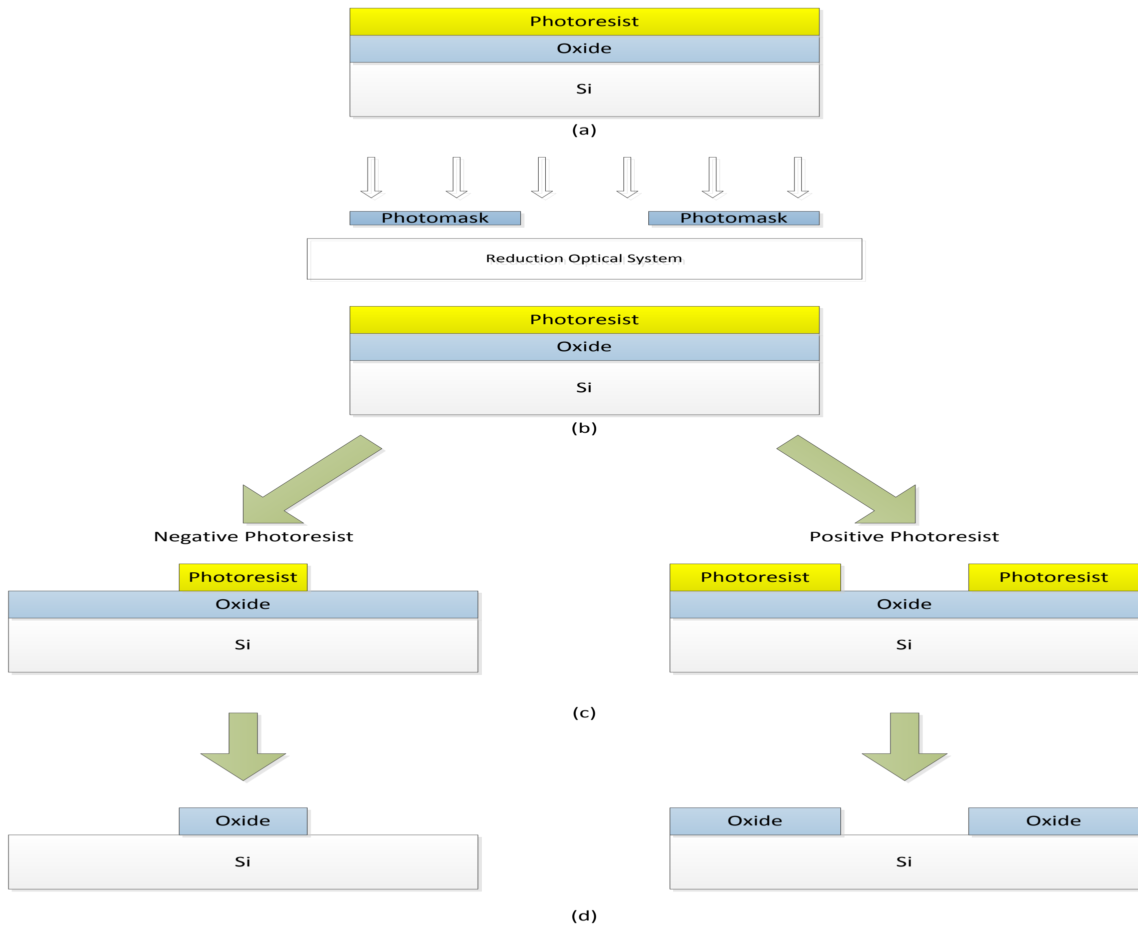

Figure 1 Major steps in the photolithography process. (a)photoresist spincoating. (b)exposure. (c)development. (d)after oxide etching and resist strip.
Minimum feature size (also called the critical dimension) of the photolithography

One factor is depth of focus of lithography projection system. As the wavelength of the light source shrinks, the depth of focus (DOF) also shrinks. A small DOF limits resist thickness and topology on the substrate surface. A depth of focus (DOF) follows this equation:

$$\text{DOF(depth of focus)} = k2 \cdot \frac{\lambda}{NA^2} \qquad (1.2)$$

In this equation, k_2 is another coefficient determined by processing factors. Other factor is s limitation of optical system. As the wavelength getting shorter, the larger diameter lenses are required. The difficulty of manufacturing increases as the diameters of lenses getting larger. Also shorter wavelength light source has higher energy that, thermal expansion property of the lens material should be considered in the same time. Therefore, finding proper material with small thermal expansion coefficient and with completely transparent at the wavelength is other obstacle for using shorter wavelength light source. The other factor is a development of photoresist which is sensitive in certain wavelength. For these reasons, reducing wavelength of the light source is limited.

Reducing wavelength of the light source has limitation that several techniques are developed to minimize feature size further with given light source wavelength: phase shift mask lithography (PSM), immersion (Wet) lithography, and multiple patterning lithography(ML).

The concept of PSM is shifting phase of light by 180° in every other aperture by adding shift materials on the mask. Shift materials have a thickness, which satisfies $t= \lambda/[2(n-1)]$. Tails of the diffracted light of adjacent features cancels each other through a phase shift mask. This effect improves the modulation transfer function dramatically that resolution of the process improves significantly. The concept of PSM is displayed in Figure 2.[1]

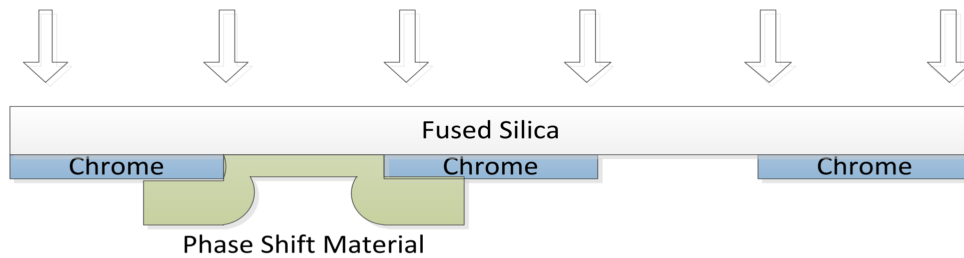

Figure 2 Concept of phase shift mask (PSM) technique.

Immersion lithography achieves minimum feature size reduction by inserting liquid between lens and the substrate. The gap had NA value as one conventionally, however by inserting liquid with higher NA (n=1.43 for water), we can achieve smaller minimum feature size without changing light source. In the higher NA medium, depth of focus also improves due to the angle of propagation decreases that critical dimensions exposed to the light with higher uniformity. [2]

Double patterning is the simplest case of multiple patterning lithography (ML). There are basically two methods for the double patterning. One is using dual tone photoresist which is cured both in the highest doses and the lowest doses of the single exposure. And the other method is patterning twice with different photo-masks. With multiple patterning method higher resolution can be achieved with same wavelength light source.[3, 4]

In Figure 3, International Technology Roadmap for Semiconductors (ITRS) [5] summarizes current technology level and future roadmap for lithography development. Currently 22nm feature size devices are manufactured with ArF eximer laser (193nm) source combined with immersion and double lithography techniques. However, solution

for patterning smaller feature size than 22nm with optical lithography is not yet developed and we are skeptical about the possibility of the optical solution. There are several alternatives are introduced to achieve below 22nm feature size: EUV lithography, E-beam lithography and nanoimprint lithography (NIL).

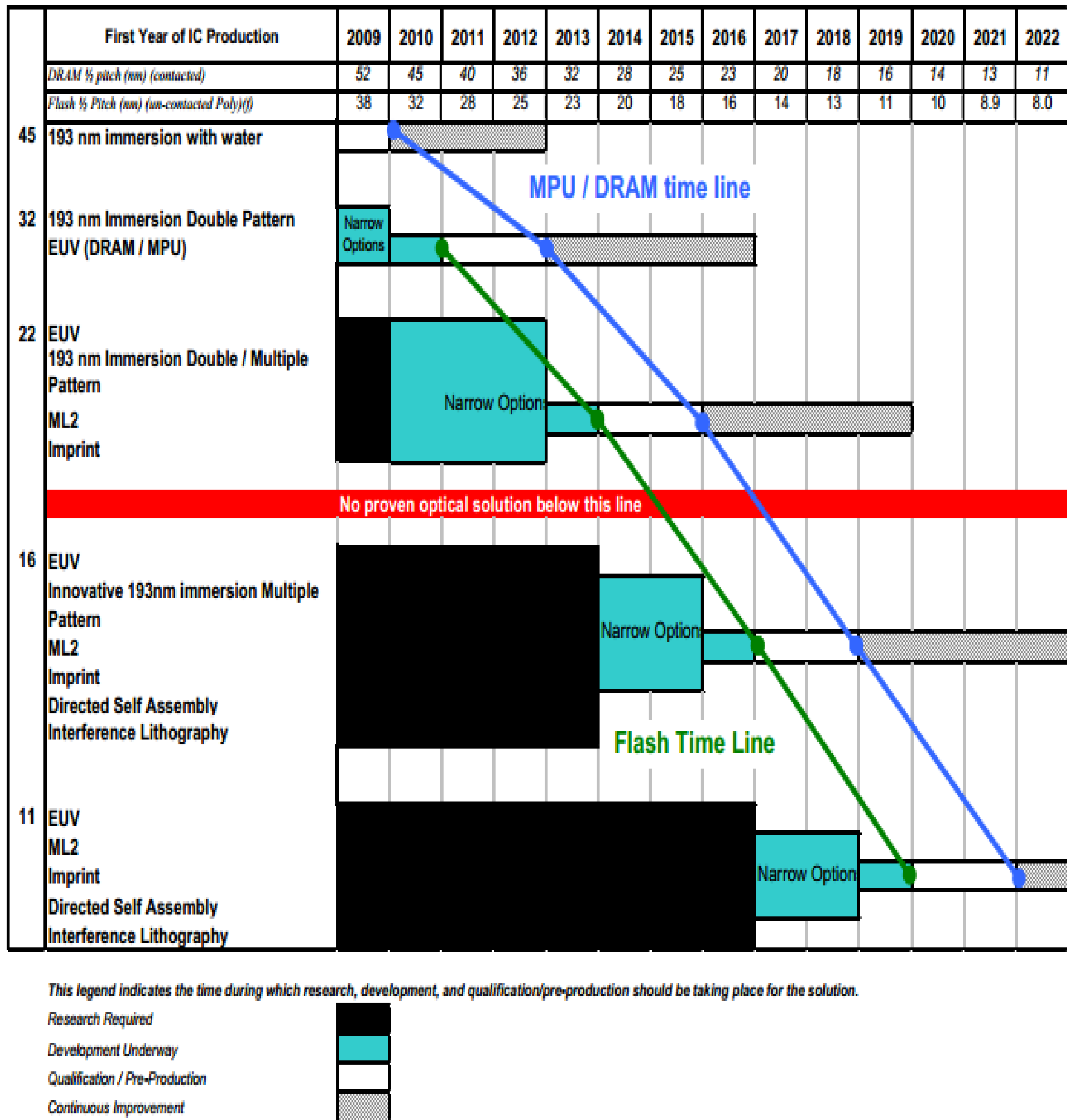

Figure 3 Lithography exposure tool potential solutions. (ITRS 2009)

The extreme ultra violet(EUV) lithography process adopts light source in extreme UV range(10nm-14nm) which is much shorter than photolithography light source wavelength(λ~150-200nm) to achieve smaller feature size. As explained earlier, conventional optic system does not operate well with extreme UV light. Therefore, EUV lithography systems use reflective optic system, which concentrates and guides the light source with reflective mirror. As shown in Figure 3, EUV lithography is evaluated as one possible solution for sub-20nm fabrication. However its unsolved problems such as high cost installation of EUV systems and remaining technical challenges such as developing defect free EUV masks, EUV sensitive resists and stable reflective optic systems obstacle its further improvement and popular use in the industry.[6-8]

Another solution is electron beam (E-beam) lithography. E-beam lithography systems adopt electron beam as an energy source instead of UV light in conventional lithography systems to improve the resolution. Electron beam has much shorter wavelength (0.2-0.5Å) than UV light that E-beam lithography that it allows extremely high resolution fabrication reaching sub-10nm. The most common E-beam lithography approach is direct writing. The direct writing scheme allows E-beam lithography to generate extremely fine patterns. However direct writing approach inherits low throughput handicap. Therefore E-beam lithography system is hard to be used for mass production, but mainly used for optical mask fabrication or prototyping not in the mass fabrication processes currently.

One highly possible and promising method for achieving sub-10nm resolution is nanoimprint lithography (NIL) invented by the Chou group.[9-11] The resolution of NIL

depends on mechanical contact and deformation of the resist material. Therefore unlike other lithography systems, NIL is not bound to the wavelength of the light source and is immune to the light diffraction problem. Its high throughput inherited by parallel printing, low cost fabrication processes and simple equipment set-up features make NIL more attractive for next-generation microelectronic manufacturing.

There are two types of nanoimprint schemes. One scheme is thermal NIL process which utilizes heat to soften the resist layer. The other scheme is UV imprint lithography which utilizes UV light to cure resist layer.

The major steps of the thermal NIL process are illustrated in Figure4. First, a hard mold is pre-fabricated by traditional microelectronic processing, which has nano-scale features on the surface. The substrate surface is coated with polymer resist. Second, the mold is pressed into the resist layer under controlled pressure and temperature. Third, the mold is removed from the resist layer after cooling down. Thickness contrast of resist layer is created through this step. Pressed resist area with mold protrusion region will leave a thin residual layer. Therefore to achieve fully patterned resist, reactive ion etching(RIE) step is needed to remove the residual layer.

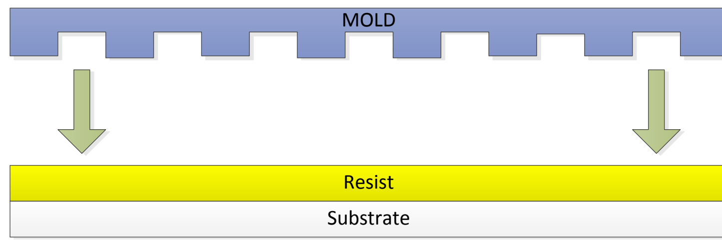

(a) Imprint (Press Mold)

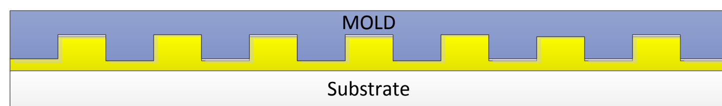

(b) Apply Heat(Thermal Cure)

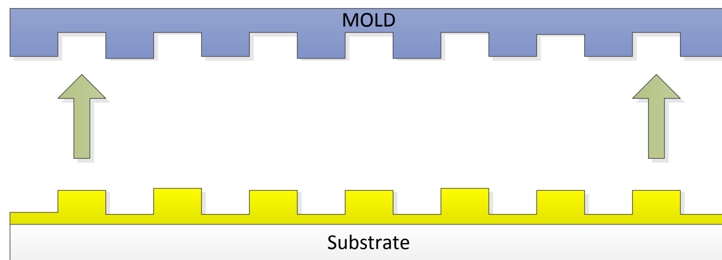

(c) Remove mold

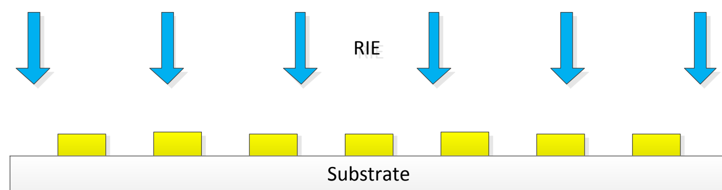

(d) Remove residual layer with RIE

Figure 4 Major steps of thermal NIL process.

UV nanoimprint process is similar to the thermal NIL process. The major steps of UV nanoimprint process are shown in Figure5. The first step is preparing transparent pre-fabricated mold. Unlike NIL process, UV nanoimprint mold should be transparent to cure the liquid precursor resist. UV curable resist is then dispensed and pressed by the mold in the following step. The fourth step is separating mold from the UV cured resist. Replica of the template pattern is formed on the resist layer. However a residual layer is also formed in UV namoimprint process below the protrusion region of the mold. Therefore oxygen plasma etching step is employed to produce fully patterned resist layer. Even though UV namoimprint process uses UV light, this process is not limited by light diffraction and beam scattering problem, deteriorates pattern resolution in traditional optical lithography technique.

Because of its simplicity the nanoimprint technique has been adopted to various applications in electronics, photonics, magnetic devices, nano-scale control of polymer crystallization, and biological applications.[12]

Nanoimprint lithography is high-throughput process, however still more research is required to meet the demands of practical applications.[13] Currently, several methods to achieve practical level of throughput are introduced: roll-to-roll nanoimprint lithography(R-NIL) and Laser assisted nano-imprinting.

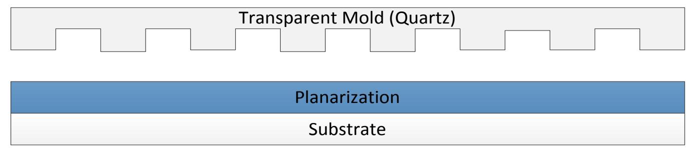

(a)Prepare Transparent Mold and Substrate

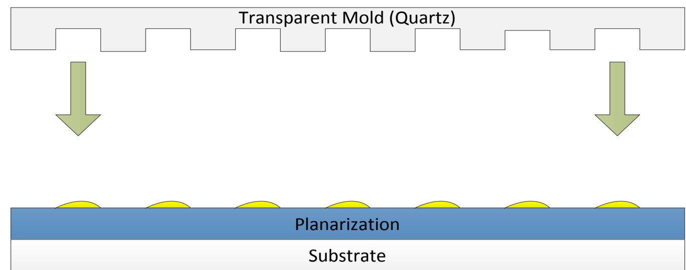

(b)Dispense UV curable resist on the prepared substrate

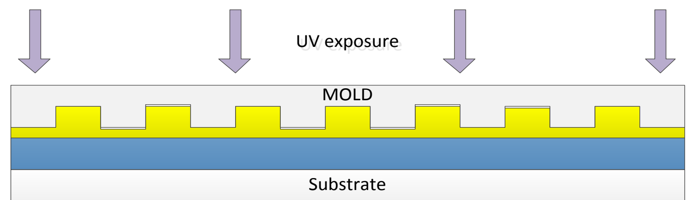

(c) Close gap and expose UV light

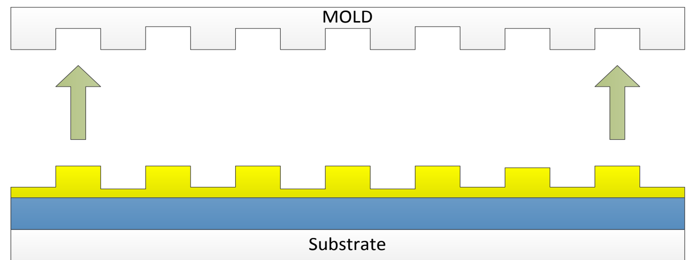

(d) Separate the Mold from the Substrate

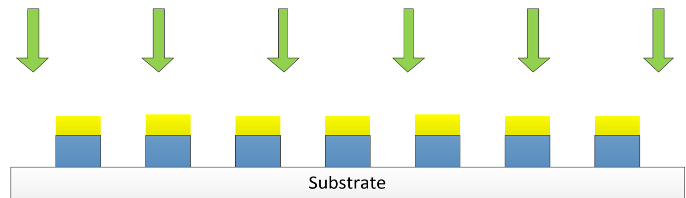

(d) RIE residual layer and etch substrate

Figure 5 Major steps of UV nanoimprint process.

Roll-to-roll nanoimprint lithography is introduced as an alternative approach to flat NIL. Compared to NIL process, R-NIL shows advantage in higher throughput, better uniformity with less press pressure and capability of large area printing.[13]

Two methods of R-NIL were initially introduced. One method is the cylinder mold method and the other method is flat mold method.[14] The cylinder mold method uses a thin metal film mold and attach around the roller surface. Therefore the roller and the mold are combined. The second method is flat mold method. In this method, the mold is similar to the conventional NIL mold, however the pressure is applied through the roller in a confined area at a time. In this method, flat mold is placed directly on the substrate, and roller rolls on the flat mold. When roller passes on the substrate, the pressure is transferred to the resist under the mold. In both methods, the roller temperature is set higher than the glass transition temperature (Tg) of the resist, on the other hand the temperature of the platform is set lower than the glass transition temperature. Therefore, only the contact area with the roller reaches a temperature above the glass transition temperature and makes the resist available to flow. In the same time, intrusion areas of the mold selectively press the resist layer until the resist is cooled down enough. Also pressure is only applied through the roller that the pattern transferring area is confined to the roller contact area. And as the roller rotates forward, this transferring area also moves and transferred pattern remains behind. Currently, successful transfer of 700nm period grating pattern has reported in papers.[13, 14]

RNIL processed pattern shows fewer bubbles than conventional NIL process due to the roller pushes the air out. NIL process was easily affected by surface unevenness

and existence of dust in the printing area because the pressure applied to the whole printing area at a time. However due to its confined pressure area, RNIL is strong to the thickness unevenness and dust existence in the printing area. Several variations of RNIL such as using UV light to cure resist are also developed.[14]

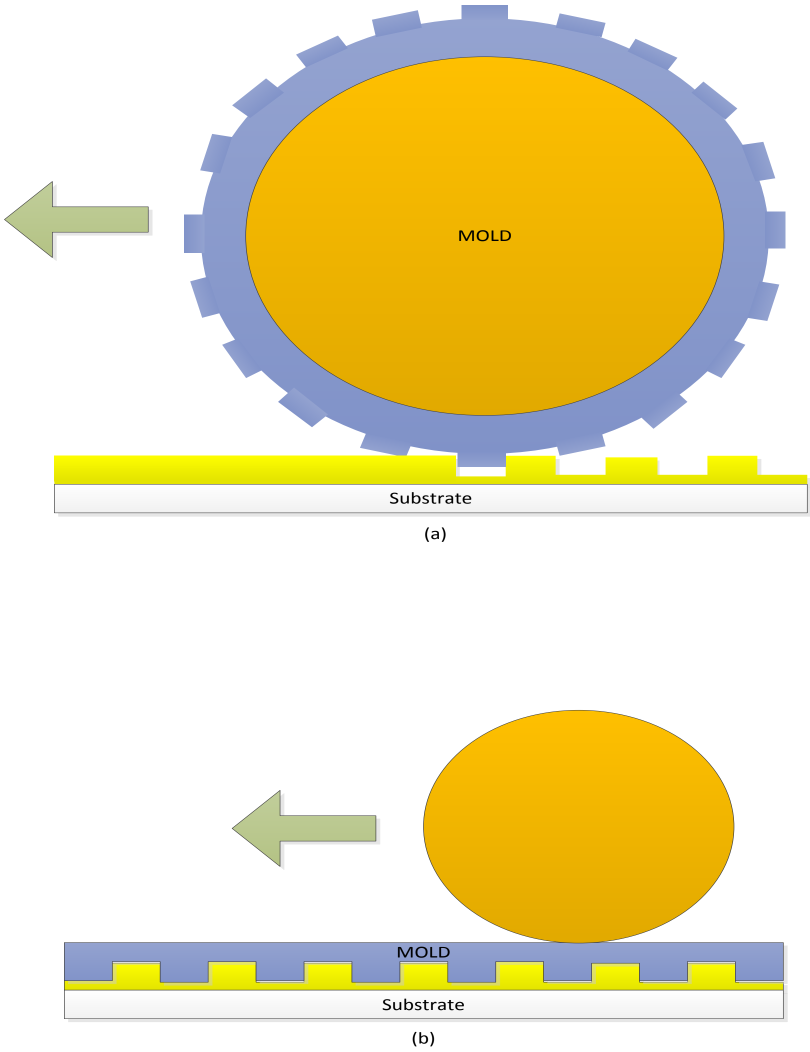

Figure 6 Two methods of roller nanoimprint lithography. (a) Cylinder mold method. (b)Flat mold method.

Another approach to improve throughput of NIL process is adopting laser to enhance process throughput. First laser assisted imprint was introduced by Dr.Chou.[15] In this technique, etching step is removed through direct printing approach. This laser assisted direct printing(LADI) method uses a XeCl single excimer laser pulse(308nm wavelength and 20ns pulse duration) to melt surface layer of the silicon substrate.

Steps of the LADI process are illustrated in Figure 7. Firstly, contact transparent quartz mold and the silicon substrate. Second, radiate excimer later to melt a thin surface layer of silicon substrate. A transparent quartz mold is required in this process due to the laser should be able to penetrate the mold and melt down the silicon substrate. The transmittance of the quartz mold for the laser radiation is measured 93%, which is almost transparent to the laser. When silicon surface melts, reflectivity of the silicon surface increases in the visible light range. Therefore, the melting of the silicon surface can be monitored by measuring surface reflectivity to the visible light change during the process. Third step is applying pressure when silicon surface melted. Due to the pressure, the pattern engraved on the mold will be embossed on the molten silicon surface. The cooling step and separation step of the mold and the substrate is followed to finish the process.

A successful fabrication of 300nm period grating pattern with LADI process was reported in the paper.[15] LADI shows advantage in short processing time (sub 250nm), high resolution (sub 10nm), and excellent imprint of large area isolated patterns. However the difficulty of the quartz mold fabrication limits its usage.

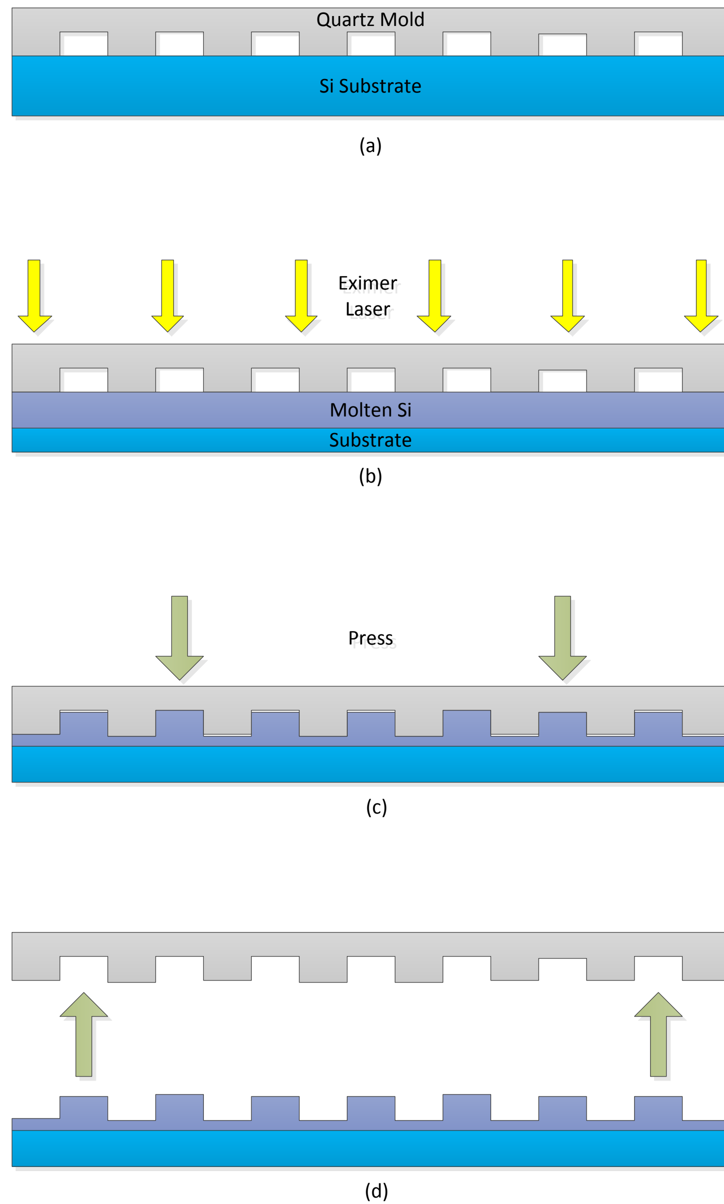

Figure 7 Steps of LADI process. (a) Contact quartz mold and silicon substrate. (b) Exicmer laser irradiation. (c) Silicon embossing and cooling. (d) Separate mold and substrate.

To overcome the difficulty of the quartz mold fabrication, IR laser-assisted imprint (IR-LAI) method was introduced. In this method, IR laser is used for lithography not direct printing on the substrate. In IR-LAI scheme, the IR laser heats the mold first,

and the heat is transferred to the stamping layer(SU-8 5). When temperature reaches above glass transition temperature of the SU-8 5(50C), applied pressure on the mold deforms the surface of the SU-8 5 layer and the pattern is transferred. Compared to conventional NIL process, IR-LAI shows advantage in processing time, and large area imprinting. Also this method uses silicon mold that it avoided the quartz mold problem. [16]

The combination of laser-assisted imprinting method and roller imprinting method was also tried. The concept of roller imprinting based on focus infrared heating is shown in Figure 8. In this method, glass roller is used to focus infrared light source. A focused infrared laser heats stamping layer(PMMA) up to glass transition temperature within very short time. And the pressure applied through the roller presses the flat mold and the pattern is imprinted on the PMMA layer. This method can imprint with higher speed and achieved wider area of imprinting than conventional imprint method. [17]

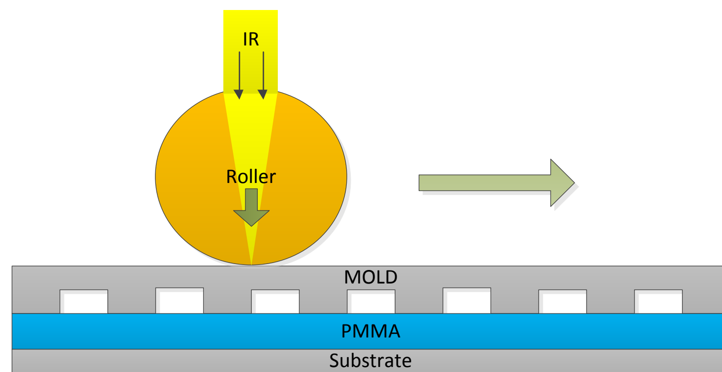

Figure 8 Concept of roller imprinting based on focus infrared heating.

CHAPTER II

PROBLEM STATEMENT

Organic electronics are currently receiving attention in research area and in commercial world due to its ultralow-cost, lightweight and its application to flexible electronic devices. Already display devices using organic light emitting devices(OLEDs) are commercially available and noticed for its high-efficiency, bright and colorful thin display. Even flexible displays are introduced for near future commercial product. Also continuous progresses are reported in organic thin-film transistors(OTFTs) and thin-film organic photovoltaic cells for the realization.[18]

The cost of the organic materials used in organic electronics are low, however the price of the organic electronic devices are mainly dominated by its fabrication and packaging costs rather material cost. Therefore, developing low-cost organic device fabrication methods on inexpensive, large-area substrates are highly demanded.

With silicon based semiconductor devices, photolithography process has been most powerful and widely used fabrication method. As explained in previous chapter, photolithography process consisted of many steps exposing to corrosive reagents, plasmas, and high temperature. Those strong stimulating processes are suitable for robust inorganic semiconductor production. However, it is hard to apply to the organic materials in general which are soft and fragile. Therefore different approach is required for organic device fabrication. Several processes are currently introduced for organic semiconductor fabrication. Those can be categorized in four groups: solution deposition

of polymer thin film, vapor phase deposition of small molecules, thermal transfer of organics and direct printing.[18]

Methods in solution deposition of polymer thin film group, polymers are uniformly deposited on the substrate through spin-on or spray-on methods in general. These two methods have advantages in deposition speed and large deposition area. However, multi-layer deposition is limited due to the solvents in each step and local patterning is unavailable. Another method in this group is inkjet printing, which is one of the promising methods for the organic semiconductor fabrication process. Droplet of the polymer solution is ejected through the nozzle and deposited on the pre-patterned well of the substrate. The process can be very fast, however precise mechanical control of the nozzle and accurate chemical control of the polymer is required to satisfy electrical and optical requirements for the electronic devices. Also, achieving uniform layer over the template well is unsolved problem of this technique.[19] Currently reported resolution of the inkjet printing with organic semiconductors is in between 50 - 100um. [19]

Second group of organic semiconductor fabrication methods is vapor phase deposition of small molecules. In general, vacuum thermal evaporation (VTE) method is used for the small molecule deposition. This method uses thermal sublimation of small molecules in vacuum chamber to deposit. Through the vacuum thermal evaporation method, multi -layer of the organic film is easily achievable. Also VTE is dry process that there are no concerns of solvent contamination. Nevertheless there are several shortcomings. The process dissipates excess material due to the scheme. In addition it is hard to control uniform deposition rate with the organic semiconductor because organic

semiconductors are typically thermal insulated. To overcome shortcomings of the VTE, organic vapor phase deposition (OVPD) has been introduced. This scheme uses inert carrier gas to maintain uniform deposition(Figure 9(a)).[20] Both VTE and OVPD can achieve local patterning through masking method. Typically minimum feature size corresponds to the thickness of the mask thickness (~20-75um).

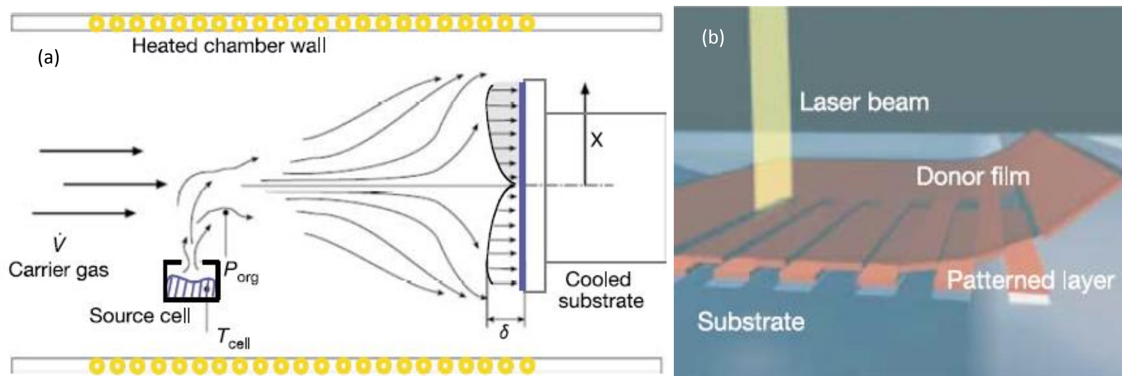

Figure 9 The process of organic vapor phase deposition(OVPD) and thermal printing. (a)OVPD. (b)thermal printing. Reprinted by permission from Macmillan Publishers Ltd: Nature, (Forrest, S.R., *The path to ubiquitous and low-cost organic electronic appliances on plastic*. 428(6986): p. 911-918), copyright (2004) (ref[18]).

Third group is thermal transfer of organics. As you see from the figure9(b), organic material coated donor film make contact with substrate. When a localized heat source or a laser beam applied, thermal transfer take place. However, this process has material choice limitation. The material should have resistance to thermal degradation and suitable mechanical properties for the thermal imaging process.

Last category is direct printing group. The pre-patterned mold directly touches the substrate and transfer the organic material. This is basic scheme of the direct printing methods. The main technique of this group is transfer printing which is shown in figure9. There are several different methods in transfer printing. The first method is subtractive

method. We prepare the pre-patterned mold coated with adhesion enhancer on the patterned side and substrate coated with uniform organic material. When the mold makes contact with the substrate and releases it, organic layer is negatively patterned on the substrate due to the adhesion enhancer layer at the protrusion of the mold. The positive method with the structured stamp is opposite. The organic layer is coated on the mold, and the adhesion layer is coated on the substrate. After the contact, positive pattern is transferred to the substrate. Third method is additive method with flat stamp. Its scheme is combination of subtractive and additive method with structured stamp. Organic patterns on the flat stamp are prepared through the subtractive transfer printing method and patterns are transferred to the substrate through the additive transfer printing method. Typically soft Poly-dimethylsiloxane (PDMS) material is used for the flat stamp. PDMS material is soft material that, this methods can be applied to the curved surface. Also there is report that transfer printing with the flat stamp showed less shape distortions of the pattern due to the edge effects on structured PDMS stamp. More details of the additive method using flat stamp is shown in figure10. With flat stamp transfer printing, successful transfer of 50um wide P3HT:PCBM blend line pattern is reported.[21]

We reviewed the existing fabrication processes for the organic semiconductors. We still need suitable organic semiconductor fabrication methods with low cost, high throughput, large area fabrication features. In this work, nanoimprint-based transfer imprinting of organic semiconductor is studied. This technique enables residual-layer-free patterning of organic semiconductors without mold contamination. Also it requires low pressure and temperature. Nanoimprint based transfer imprinting technique is not

only high throughput process itself, but also it has further throughput improvement potential, because this technique amenable to roll-to-roll process.

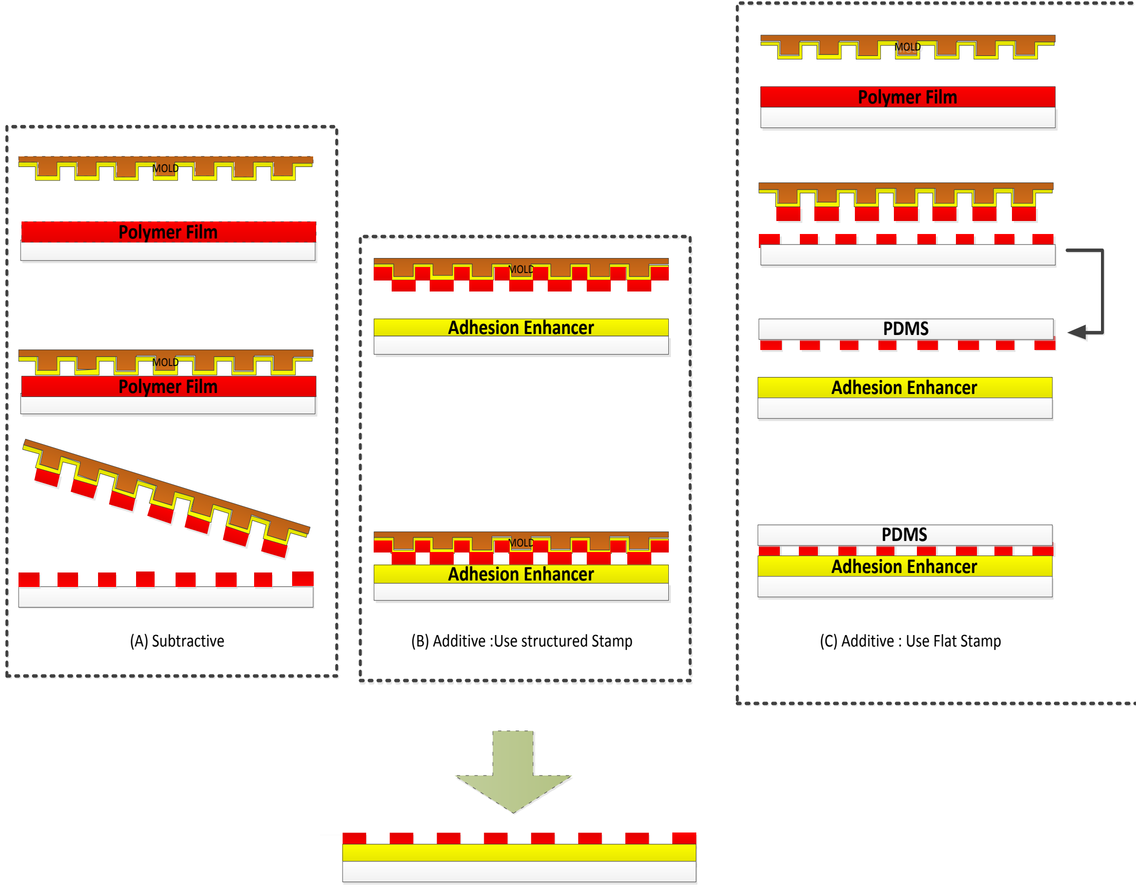

Figure 10 The schematic of transfer printing. (a) Subtractive method (b) Additive method with structured stamp (c) Additive method with flat stamp.

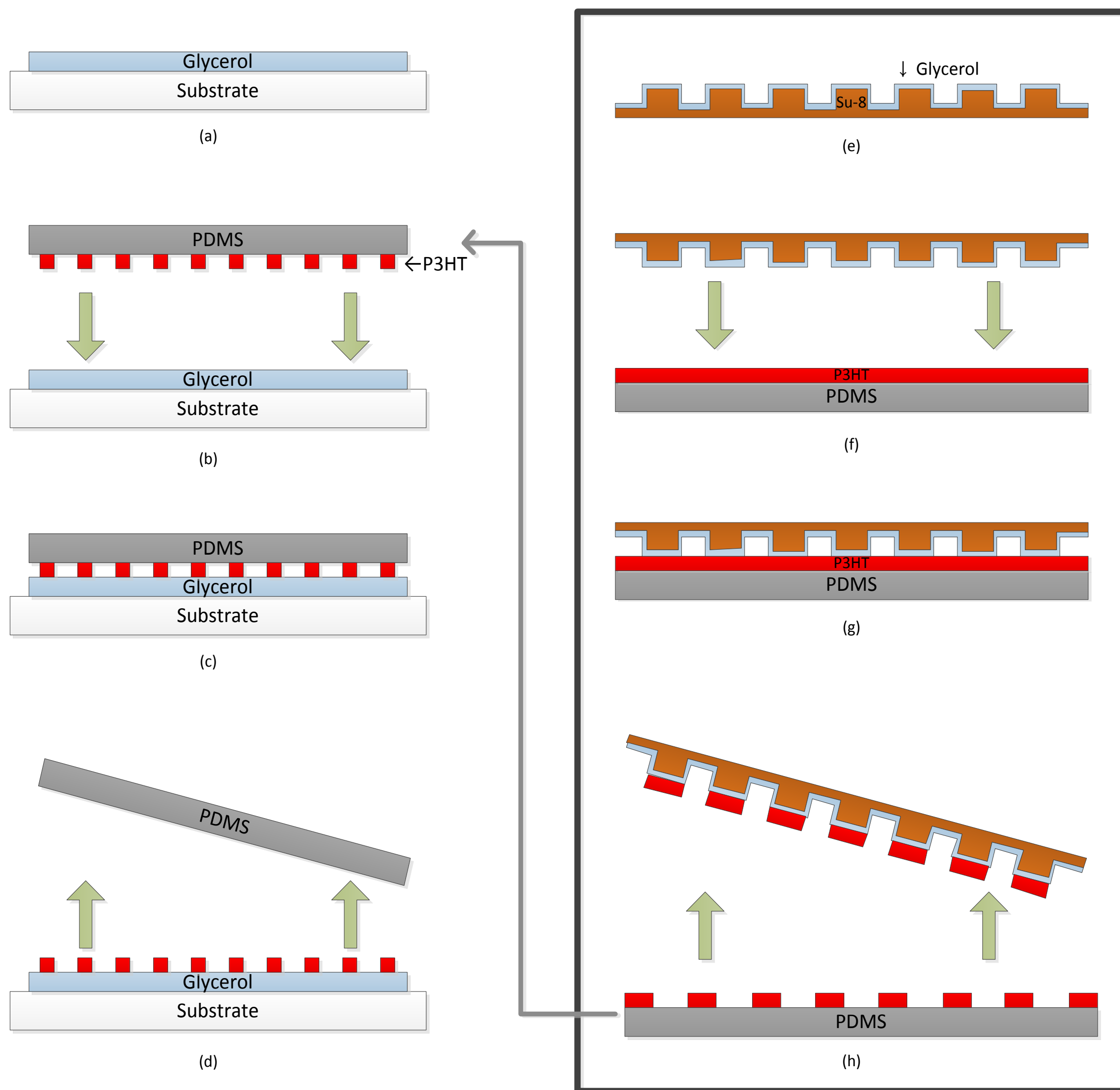

Figure 11 Steps of soft stamp polymer transfer printing. (Additive method with flat stamp) (a) Coat glycerol on the glass substrate (b) Contact P3HT patterned PDMS stamp on the substrate. (c) Apply heat on a hot plate. (d) Remove PDMS layer. (e)Prepare negative patterned SU-8 template and coat with glycerol. (f) Deposit a uniform layer of P3HT onto a flat PDMS stamp. (g) Make contact SU-8 template with PDMS film and apply heat (h) Remove the SU-8 template

CHAPTER III

NANOIMPRINT BASED TRANSFER PRINTING

3.1 PROCESS DESCRIPTION

We developed nanoimprint based transfer printing. As we can infer from the name of the technique, a suggested technique is based on a nanoimprint lithography scheme. The difference is PDMS carrier film in between the mold and the substrate. The schematic of the process is illustrated in figure12. First, we prepare pre-patterned mold. In our experiment, we used 50um, and 25um silicon mold with deep trench (20&50um). Deep mold is used to secure enough space for the pushed PDMS film during the process. A bare silicon substrate is coated with adhesion layer and we also prepare organic layer coated PDMS carrier film. We place PDMS carrier film in between the mold and substrate. Second, the mold makes contact with the substrate and pressure and heat is applied for the organic material transfer. During the imprint process, we apply uniform pressure on the mold. However, pattern on the mold selectively transfer the pressure to the surface of the substrate through the deformed PDMS film. Mold protrusion areas feel high pressure and the trench area feel low pressure. This pressure difference on the substrate surface allows selective transfer of the organic material on the substrate. Third, we release the mold and lift off the PDMS carrier film. Due to the adhesion layer on the substrate, positive organic patterns are transferred on the substrate and rest of the organic layer will be removed with the PDMS film.

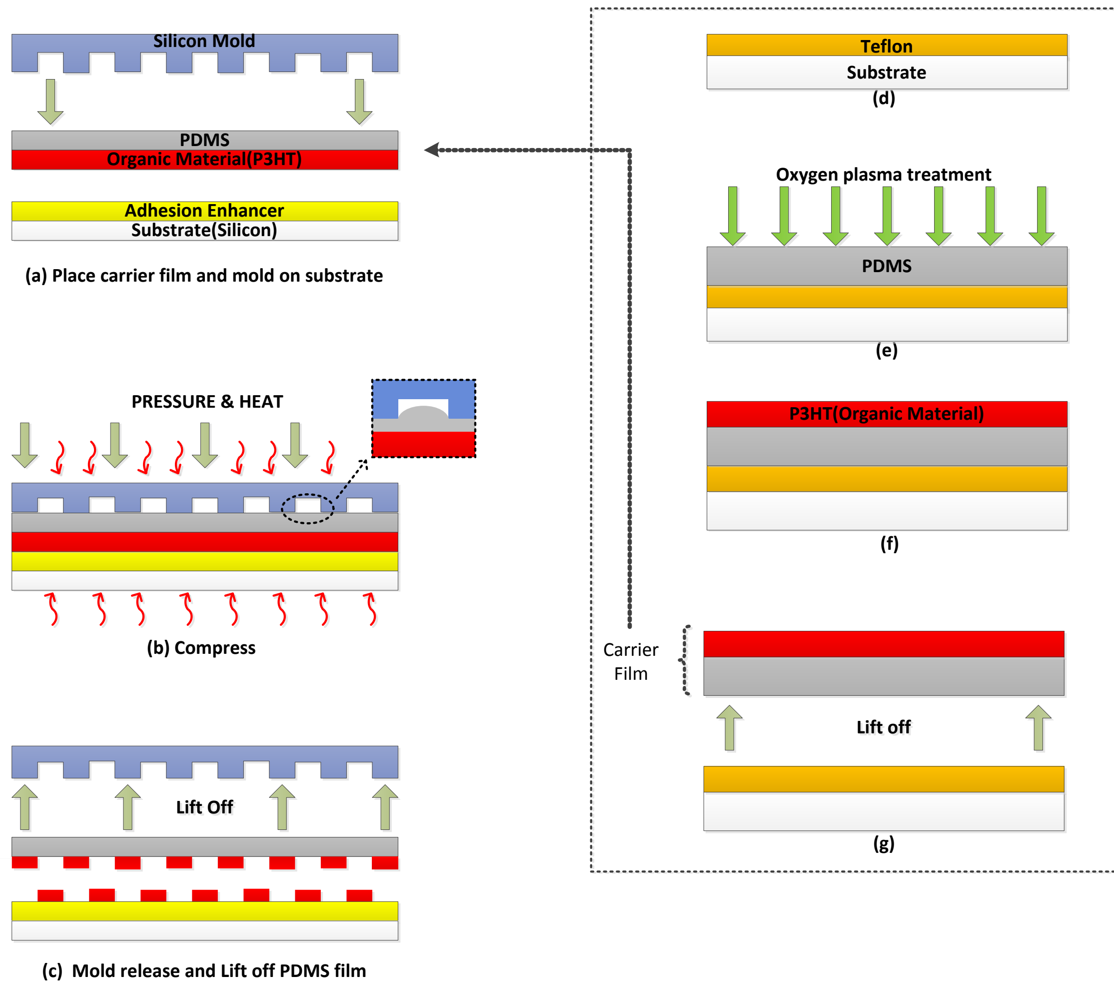

Figure 12 A schematic of the nanoimprint-based transfer printing. (a-c) nanoimprint based transfer printing steps (d-g) carrier film preparation steps.

3.2 EXPERIMENTAL DETAILS

3.2.1 ADHESION ENHANCE LAYER

In this work, we used Poly(3-hexylthiodphene-2, 5-diyl) (P3HT) for the organic material layer. However, P3HT has poor adhesion to the silicon substrate. Several material has been tested for the adhesion layer and Cyclotene AP3000(advanced electronic resins, DOW) showed best result with the process. Cyclotene AP3000 is

widely used for bonding material in micro-scale fabrication because of its good planarization and no outgassing features. The details of the material will be discussed in the material section. The organic portion of the material improves adhesion toward organic polymers that Cyclotene is suitable for our process. Also we can achieve pretty thin (sub 100nm) adhesion enhance layer with Cyclotene solution which is desirable to the process.

3.2.2 CARRIER FILM PREPARATION

We used PDMS material for the carrier film. PDMS film not only does a role as an organic film carrier but also the separation layer to prevent mold contamination. The steps of PDMS carrier film preparation is shown in figure11(d-g). First step is spin-coating Teflon layer on the silicon substrate. A 2%wt Teflon AF, amorphous fluoro-polymer resin in fluorinert electronic liquid(FC-40, 3M company) was used for during the spin-coating step and we achieved ~200nm thick Teflon layer. A Teflon layer reduces the adhesion between PDMS film and the substrate that it allows damage free separation. With the Teflon layer, damage free separation of sub 1um PDMS film is reported. [22] Second step is spin-coating PDMS layer. PDMS(Sylgard 184, Dow Corning) is mixed in 10:1(base:cure agent) ratio and degassed in vacuum chamber. After degassing, PDMS film is spin-coated on the Teflon layer and thermally cured in the oven(150°C, 1hr). Several spin-coating speeds were tested to achieve different PDMS film thicknesses. Third step is oxygen treatment on the PDMS surface. Without any treatment, PDMS film shows hydrophobic that achieving uniform organic layer is not

possible with spin-coating. Therefore, additional step for the PDMS surface property modification is required. After oxygen treatment, PDMS surface changes to hydrophilic for several hours. Fourth step is P3HT layer deposition through spin-coating. A 2%wt P3HT solution in 1,2-dichrobenzene is used for the P3HT layer deposition, and achieved ~80nm thick P3HT layer. In this step, spin-coating time was extended to eliminate solvent instead of the soft-bake. Because under high temperature, PDMS film surface changes back to hydrophobic that work of adhesion between P3HT layer and the PDMS film is also affected. When we compared the result, solvent removal with long spin-coating time showed better transfer result. Last step is lift-off carrier film from the substrate. We inserted Teflon layer that PDMS film can be separated from the substrate easily. However, less than 10um thick PDMS film, it rolls up easily. Therefore making frame along the edges of the PDMS film with double sided tape helps to handle thin PDMS film. This method also reduces formation of the wrinkle when we place the PDMS film on the substrate(figure 11(a) step). In this method, we physically separate the carrier film. However PDMS carrier film can be prepared through the chemical conditioning. In this method, we replace Teflon layer with sacrificial layer such as Poly(methyl methacrylate) (PMMA). By dissolving the sacrificial layer with the solution, we can separate PDMS film without stress. Also PDMS film placement on the substrate can be processed through the solutions. This chemical method allows damage free sub 1um PDMS film separation. However in this study, physical separation method has mainly used due to the easiness of the process and to reduce the possibilities of organic layer contamination.

3.2.3 QUANTITATIVE EXPERIMENTS

To optimize the process condition, we performed quantitative experiments under different imprinting conditions. The process variables were imprinting pressure, temperature, time and PDMS film thickness.

Table 1 Quantitative experiment variables & ranges.

Process variables	*Tested range*
Pressure	12.5 - 100 (psi)
Temperature	25 - 150(°C)
Imprinting Time	10(sec) - 10(min)
PDMS film thickness	5 - 30(um)

3.3 MATERIALS

3.3.1 PDMS

Polydimethylsiloxane (PDMS) is one of the most popular silicone-based polymers in microfluidics. The advantage of PDMS such as easy handling, low cost, biocompatibility, chemical inertness, optical transparency, elastomeric property, and gas permeability are attractive for rapid prototyping in microfluidic devices. Also due to its easy handling and low cost properties, PDMS is popularly used as micro-contact printing stamp material.

Even though PDMS has many advantages, untreated PDMS is hydrophobic material that it restricts wide use in applications. The chemical structure of the repeating

O-Si(CH3)-O units are the reason for the hydrophobic PDMS surface. It is reported that oxygen based plasma treatment reduces hydrophobicity of PDMS surface. The plasma treatment removes methyl(Si-CH3) groups and introduces silanol(Si-OH) group that the treated PDMS surface converts from hydrophobic into hydrophilic for a few hours after plasma treatment. This oxygen-based plasma modification of PDMS surfaces is widely used to attach PDMS micro-channels in microfluidic devices or to change the surface property of PDMS stamps in micro-contact printing.

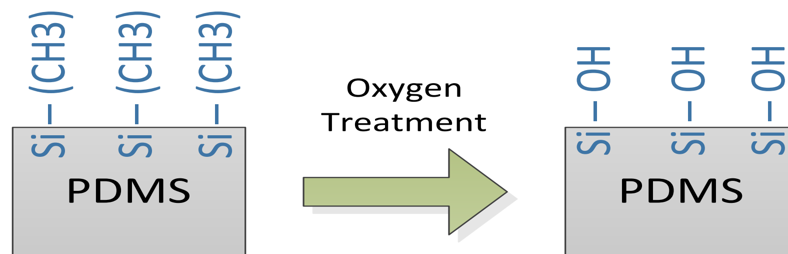

Figure 13 PDMS surface modification.

In our project, PDMS(Sylgard 184, Dow Corning) is used for the organic material carrier film. PDMS base is mixed in 10:1 ratio with its curing agent. Also oxygen plasma treatment is used to coating organic material on the PDMS film surface.

3.3.2 CYCLOTENE AP3000

Cyclotene AP3000 (advanced electronic resins, Dow) is a resin prepared from B-staged BCB(bixbenzocyclobutene-based) monomers. Cyclotene is generally used for microelectronic device fabrication for dry-etching protective layer, or photoresist. Cyclotene resin is also widely used for bonding material or adhesion enhance layer

because of its good planarization and no outgassing properties. The chemical structure of BCB is shown in figure14. When Cyclotene is spin-coated on the silicon substrate, organo-silane covers the surface with the organic portion facing outward.[23] In our process, the organic portion of the BCB promotes the adhesion toward the organic polymers which is beneficial.

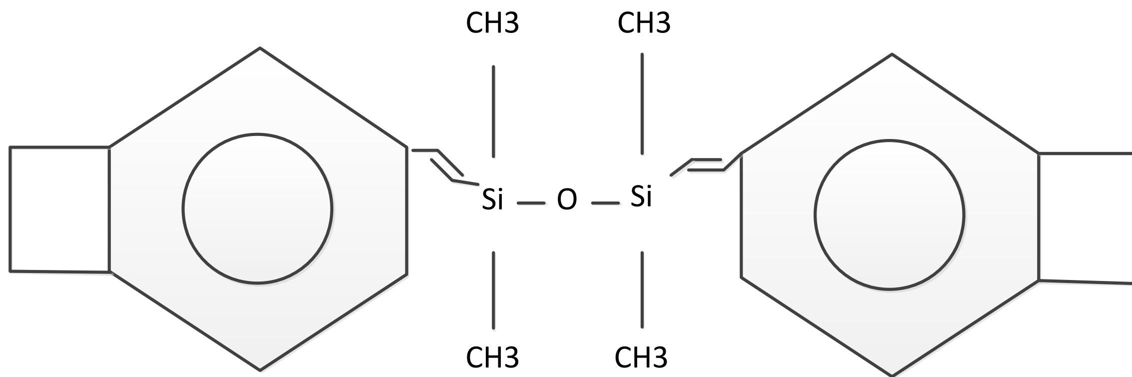

Figure 14 Chemical structure of Cyclotene. [24]

Also with diluted Cyclotene solution in Propylene glycol methyl ether acetate (PGMEA), sub 100nm BCB layer was achieved with spin-coating. The measured adhesion layer thickness on silicon substrate under different dilute ratio is shown in table2. Thinner adhesion layer is advantageous because it gives better surface roughness after imprinting due to the less reflow of the polymer.

Table 2 Measured adhesion layer thickness on silicon substrate with different dilute ratio. (Spin-coating in 3500RPM)

Cyclotene percentage in PGMEA(%)	*Measured Range(nm)*	*Average(nm)*	*Error(%)*
100	1920 – 1970	1945	2.57
50	665-680	672	2.23
33	450-465	457	3.28
25	220-230	223	4.48
20	210-220	215	4.65
16.6	177-185	181	4.41
14.2	85-94	90	8.87

3.4 EXPERIMENTAL RESULTS

We achieved 50um and 25um P3HT line pattern with nanoimprint based transfer printing method. The microscopic image of the transferred pattern is shown in figure15. The image is taken after removing the adhesion layer with PGMEA solution. This result is achieved under 75°C process temperature, 25psi imprinting pressure and 3min pressing time condition. In figure15, P3HT lines are colored dark and it shows clear separation between the lines. Lines showed slight extension due to the PDMS thickness. When we examine transferred patterns after quantitative experiment, duty cycle of the transferred pattern is linearly increased as the thickness of the PDMS film increases (figure16). The reason will be analyzed in the discussion section.

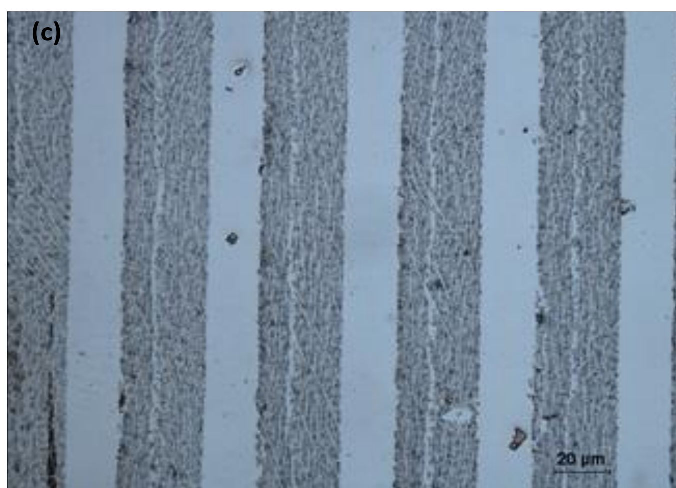

Figure 15 Microscope images of transferred P3HT patterns. (a) 50um line patterns (b) 25um line patterns (c) magnified 25um line patterns

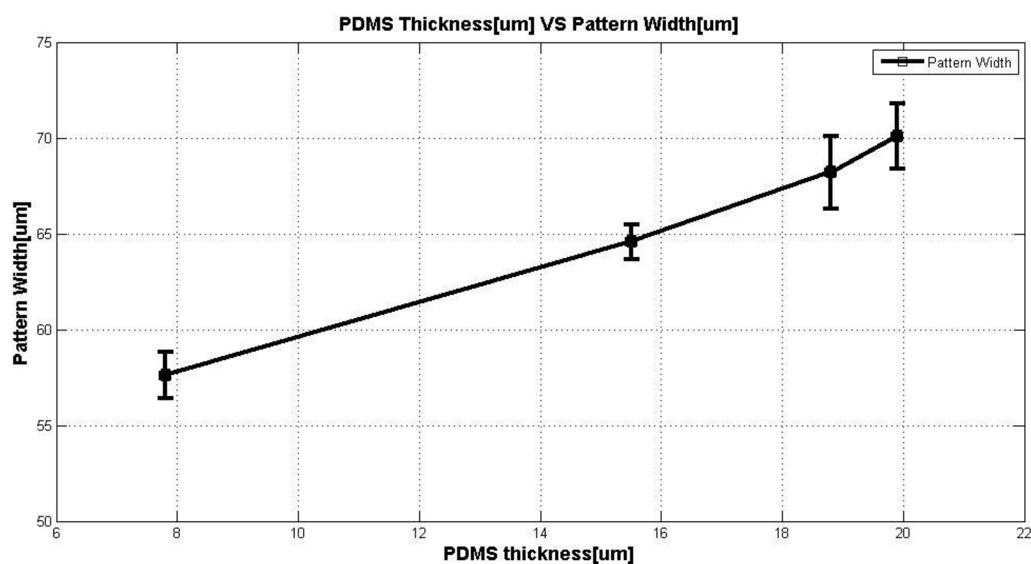

Figure 16 Transferred pattern widths with different PDMS thickness. (Imprinting condition: temperature 75C, pressure 25psi, pressing time: 3mn.)

Through the quantitative experiments we achieved optimal process range. In general, below the optimal range, transferred pattern showed partial transfer and showed whole layer transfer above the range. In between 75-100°C temperature, 25-75psi imprinting pressure, and 1-3min pressing time conditions the transfer showed best. Also above 100°C, transferred pattern showed rough line edge.

We verified transferred pattern and the process scheme. To verify the transferred pattern as P3HT, we used fluorescent microscope. According to the absorbance and emission spectra of P3HT film, absorption of P3HT showed peak at 519nm wavelength(2.19eV) and emission from P3HT showed peak at 650nm(1.88eV)[25]. To verify transferred patterns are P3HT, we used fluorescence microscope to excite transferred pattern with UV light and achieved red colored patterns (corresponds to emission peak of P3HT film) as shown in figure17(a). This image proves that transferred

pattern is P3HT. This image also shows clear separation between the lines. Figure 17(b) shows the optical microscope image of the PDMS carrier film after transfer imprinting. The light brown regions are P3HT stripes that are not transferred to the substrate and remain on the PDMS carrier film due to the absence of pressure at mold trenches. This verifies the process is following the scheme as what we designed which is selective organic layer transfer on the substrate.

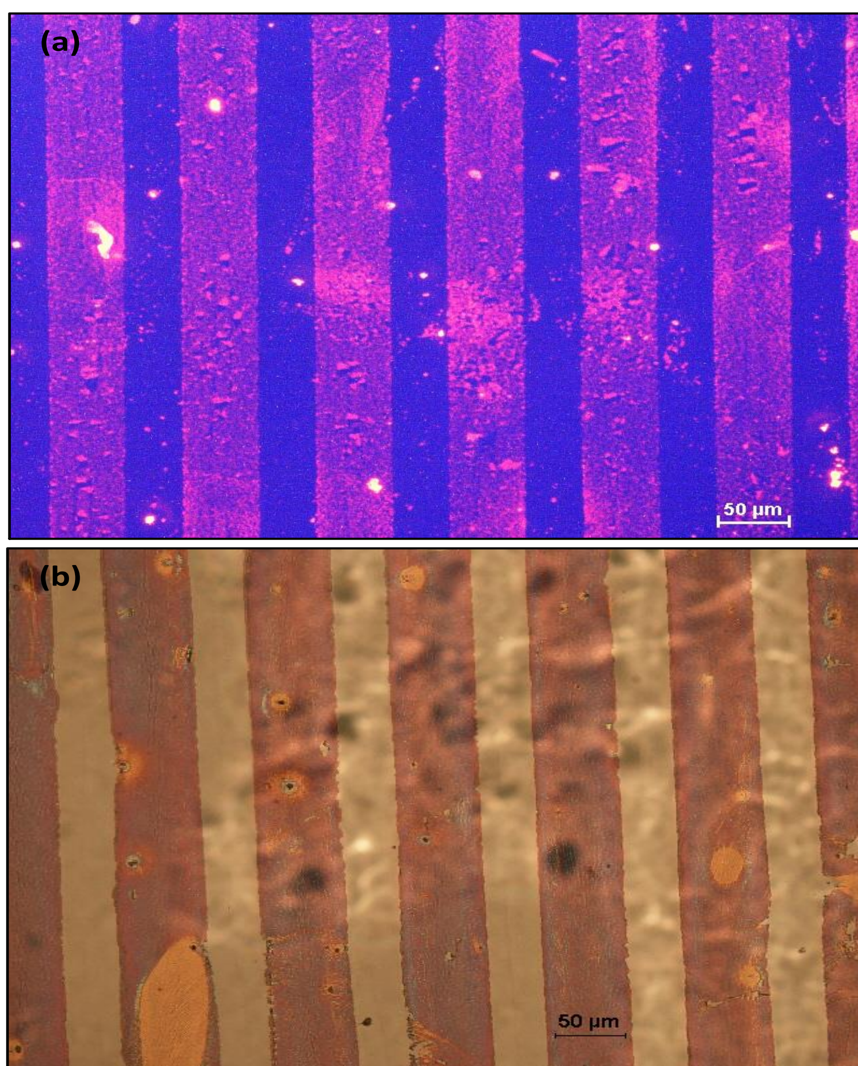

Figure 17 Images of 50um P3HT line patterns. (a) Fluorescent image of 50um P3HT line patterns. (b)Microscope image of PDMS film after the process.

CHAPTER IV

SIMULATION AND MODELING

To analyze the process we simulated the process with COMSOL multi-physics simulator. In this simulation work, we simplified the process and analyzed the process emphasis on deformation of PDMS film and pressure distribution at the surface of the substrate during the imprinting step. Variables used during the process simulations are PDMS thickness, imprinting pressure, imprinting temperature and mold pattern width.

4.1 GEOMETRIC MODELING

Geometric modeling of the imprinting step is illustrated in figure18. We modeled small area that we set periodic boundary along the x-axis. During the modeling, organic layer film and adhesion layer film are ignored. Because the thickness of the PDMS film is much thicker (5-20um) than the other films (80-200nm) that behavior of the PDMS film dominates the process whereas the influence of the thin films is insignificant.

4.2 PROCESS PHYSICS MODELING

Our simulation work is based on the COMSOL solid structure mechanics model which is for the analysis of linear elastic solid model. This model considers three equations: equation of motion (Newton’s second law), constitutive equation (Hooke’s law), and strain-displacement equations. The formula of each equation is shown in table3. PDMS film is a visco-elastic material, which shows both viscous liquid and

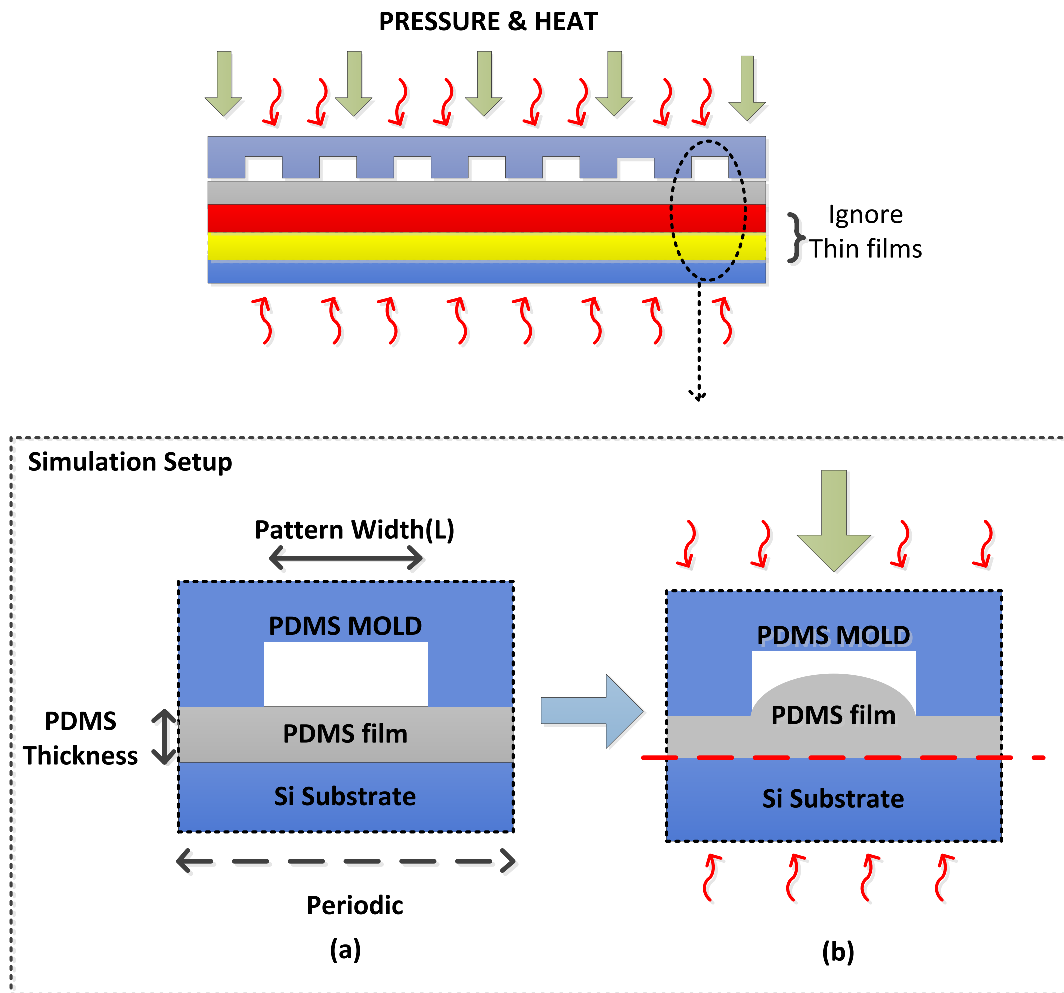

Figure 18 Geometric modeling of the nanoimprint-based transfer imprinting process.

elastic solid behavior like rubber. Therefore, we applied visco-eleastic model for the PDMS film. Also PDMS film has relatively high thermal expansion coefficient that thermal expansion model was added for the simulation. Due to the added models, constitutive equation changes from equation(4.1) to (4.2).

$$s - S_0 = C(E, \nu) : \epsilon \qquad (4.1)$$

$$\mathrm{s} - \mathrm{S}_0 = \mathrm{C}(\mathrm{K}, \mathrm{G}) : (\epsilon - \alpha(T - Tref) - \epsilon 0) \qquad (4.2)$$

Table 3 Equations of Comsol solid structure mechanics model.

Explanation	***General Form***	***Tensor Form***
Equation of Motion (Newton's second law)	$F + u\frac{dm}{dt} = m\frac{dv}{dt}$	$\nabla \cdot \sigma + F = \rho\ddot{u}$
Constitutive equation	$\sigma = E\epsilon$	$\sigma ij = Cijkl\varepsilon kl$, $\sigma = s$
(Hooke's law)	$(F = -kx)$	$s - S0 = C(E, \nu) : \epsilon$
Strain-displacement equations		$\epsilon = \frac{1}{2}[\nabla u + (\nabla u)^T]$
σ(Cauchy stress tensor), E(Young's modulus), ϵ(Strain tensor), C(stiffness tensor), ν(Poisson's ratio), u(displacement), α(thermal expansion coefficient)		

PDMS material properties used in simulation is shown in Table4. [26, 27]

Table 4 PDMS material properties

Property of PDMS	*Value*	*Unit*
Density (ρ)	965	Kg/m^3
Coefficient of Thermal Expansion (α)	3.1E-4	1/K
Bulk Modulus (G)	1.45E6	Pa
Shear Modulus (K)	0.432E6	Pa

4.3 SIMULATION RESULTS

Through the simulation we achieved PDMS deformation and pressure distribution data. Figure 19(a) shows the two-dimensional total displacement during the process. Deformation of the PDMS film during the imprinting step can be observed with this result. One of the concerns during the experiment was the mold pattern depth. We wondered thick PDMS film would touch the mold trench area when PDMS film is deformed. The simulation result (figure19(b)) shows that for the 50um pattern width, 20um mold trench depth secures enough gap between the trench and the deformed PDMS film.

Two dimensional pressure distribution is shown in figure20(a). Pressure at the surface of the substrate shows clear difference between below the mold protrusion area and below the mold trench area as we designed the process. We also plotted one dimensional pressure distribution at the surface of the substrate according to the variables (figure20(b-e)). According to the simulation result, with the thinner PDMS film, pressure shows more abrupt change and larger pressure difference between the protrusion and the trench area of the mold (figure20 (b).

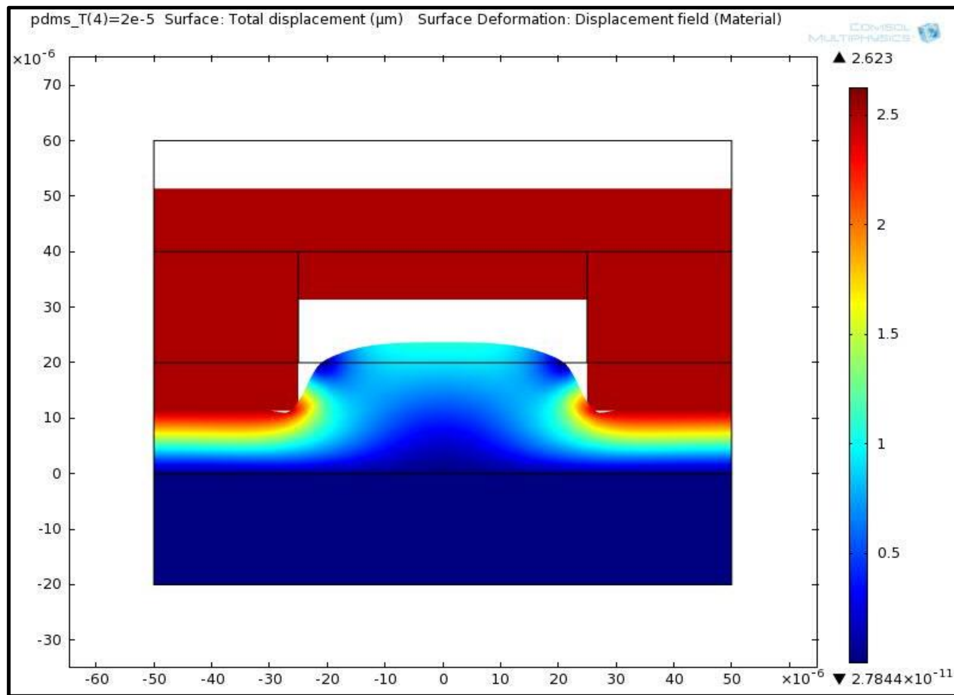

(a)

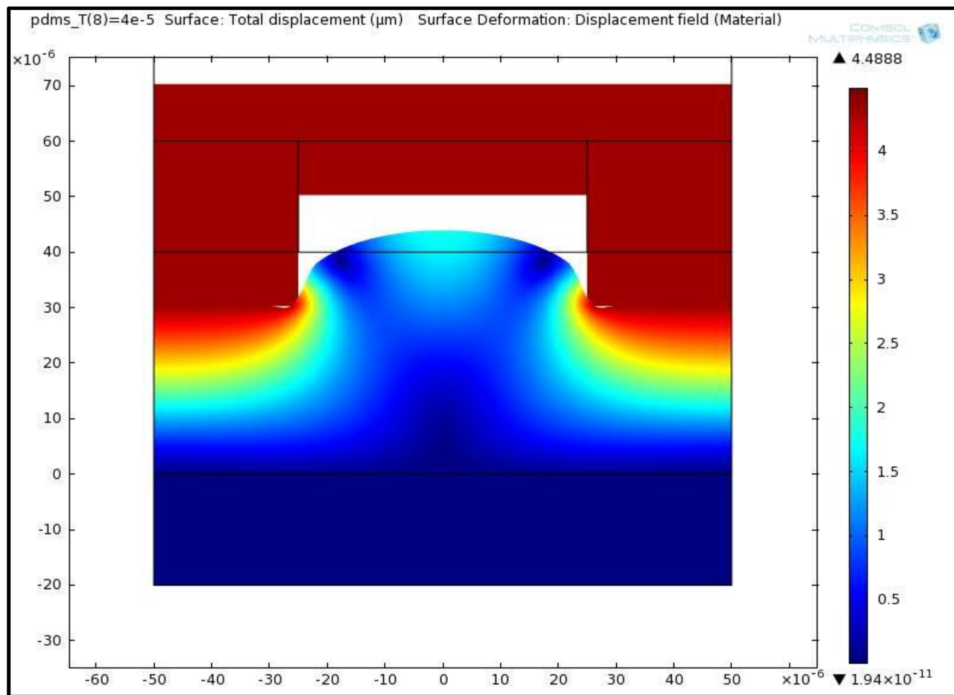

(b)

Figure 19 2-D total displacement results. (a) with 20um PDMS thickness (b) with 40um PDMS thickness.

Thus thinner PDMS film is desirable for higher resolution. This can be confirmed with the pattern width variable graphs (figure20(d,e)). The condition difference between figure20(d), and (e) is PDMS film thickness(5um, 20um). When we compare these two graphs, the process with thinner PDMS film showed larger pressure distinction. This result shows that PDMS film thickness influences on the resolution of the process. The detailed relation between the PDMS thickness and the process resolution is discussed in discussion section.

Figure20(c) shows influence of the temperature on pressure. The pressure over the entire area increased slightly due to the expansion of the PDMS material with higher temperature. When we increased the imprinting pressure, the minimum pressure at the mold trench area also increases(figure20(f)). When the minimum pressure overs the critical pressure, whole transfer takes place that the upper range of the process pressure is limited. Lower range of the process pressure is also limited by the maximum pressure on the graph.

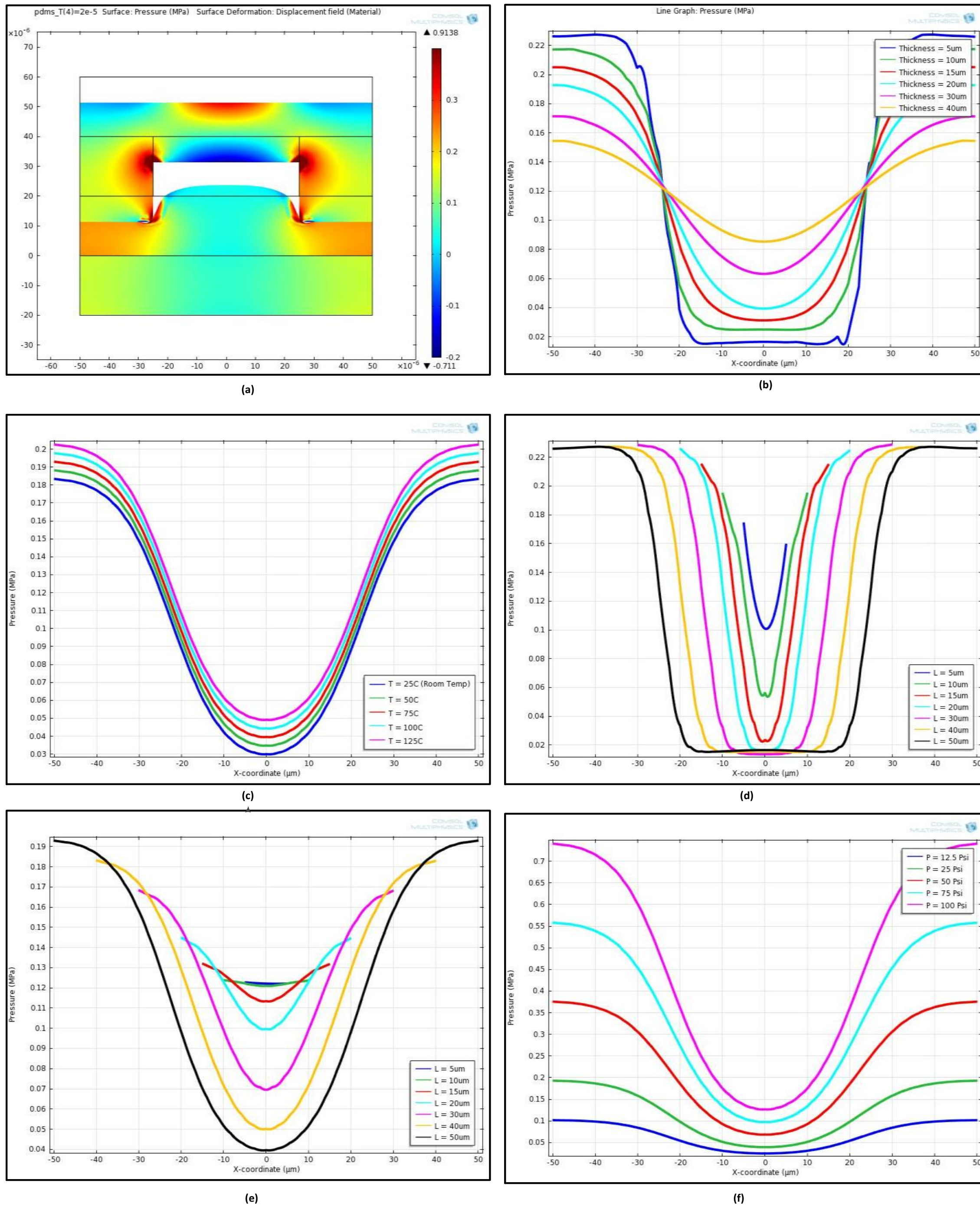

Figure 20 1-D and 2-D pressure distribution graph at the substrate surface. (a) 2-D P\pressure distribution graph with 20um PDMS thickness (b-f)1-D pressure distribution graph at the substrate surface (b)variable: PDMS thickness (c) variable: temperature (d) variable: mold pattern, with 5um PDMS film thickness (e) variable: mold pattern, with 20um PDMS film thickness width (f)variable: Pressure

CHAPTER V

DISCUSSION

By comparing the experimental results and the simulation results, we extracted critical pressure which determines pattern transfer. In figure 21, a pressure distribution graph has the same condition as experimental results(figure16). Corresponding values from the experimental results are marked on the graph and extracted the value(Table5). Due to the errors in experimental data, extracted critical pressure is given as 0.06 – 0.08MPa range. However, when we consider average values, the critical values are pretty much close to the 0.07MPa.

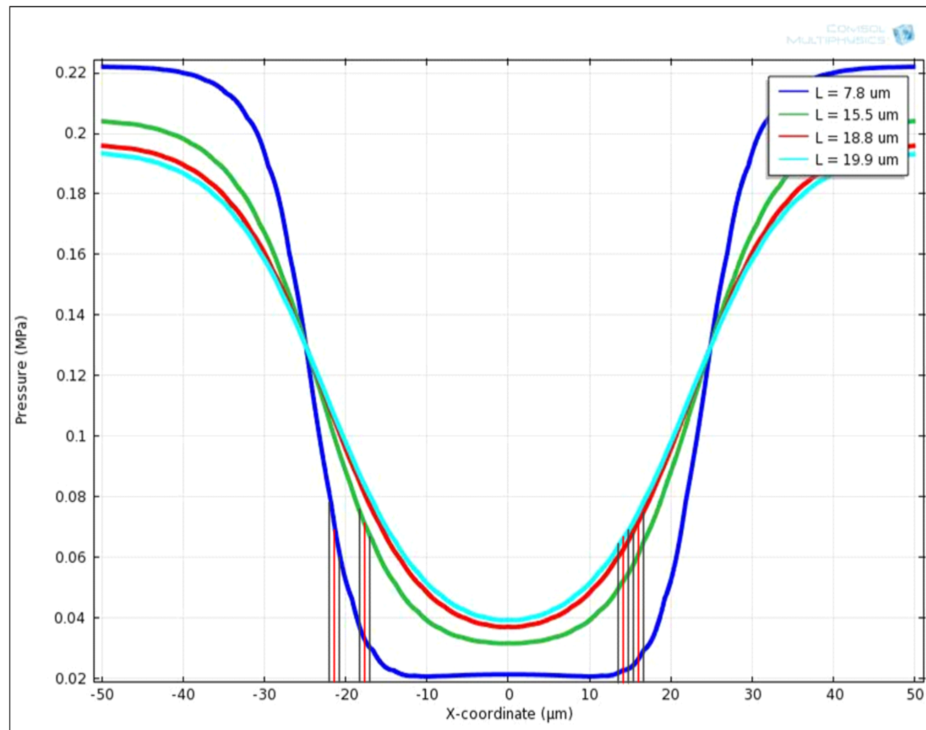

Figure 21 Simulation results correspond to the experimental results. (Figure15)

Table 5 Critical pressure extraction.

PDMS thickness	*Lower bound (MPa)*	*Average(MPa)*	*Upper bound(MPa)*
7.8um	0.079	0.069	0.06
15.5um	0.075	0.071	0.66
18.8um	0.07	0.072	0.074
19.9um	0.067	0.07	0.072

Based on the extracted critical pressure, we analyzed nanoimprint based transfer printing process. Figure21(a) shows the relation between PDMS film thickness and the minimum resolution. From the experimental results, we already found PDMS film thickness influences on the process resolution. When we look the relation in detail, they have linear relation. Minimum resolution of the process can be approximated to the 1.5 times of the PDMS thickness. When the PDMS thickness is less than 10um the linear factor increases slightly. Therefore developing ultra-thin PDMS film layer handling method will improve the process resolution further.

$$\text{Process min resolution } \approx 1.5 \text{ X PDMS thickness}$$

We also looked the relation between the duty cycle and the PDMS film thickness relation. To count on the mold pattern width in this analysis that x-axis is replaced to the ratio of PDMS film thickness and the pattern width. This relation also shows linear property. Therefore we can control duty cycle of the transferred pattern by changing

PDMS film thickness with the same mold. This feature is beneficial because this reduces additional mold fabrication for the different duty cycle.

Temperature factor increased pressure slightly due to the expansion of the PDMS film. Increased pressure results in widening of the transferred pattern. However the influence of the temperature on pattern duty cycle was not observed during the quantitative experiment because the error of the measured pattern width was larger than its effect.

From the optimal process range, we can easily catch that the process does not require high temperature or high pressure like nanoimprint lithography.

CHAPTER VI

CONCLUSION

In this work, we suggested new transfer printing method for organic semiconductors based on nanoimprint lithography scheme. The process is simple, low cost, high throughput, residual layer free. Also the mold reusability is high and the process does not require high pressure or temperature. With our suggesting process, we achieved 25um and 50um P3HT line patterns on Si substrate. The minimum resolution of the process is mainly determined by the PDMS film thickness. One more benefit of the process is that we can achieve multiple duty cycle patterns with the same mold by changing the thickness of the PDMS film which is much easier than fabricating new template. Nanoimprint based transfer printing method is compatible to roll-to-roll process that we expect further throughput improvement with the method. Therefore, nanoimprint based transfer printing technique can be applied to high throughput patterning of organic semiconductors for low cost electronic applications.

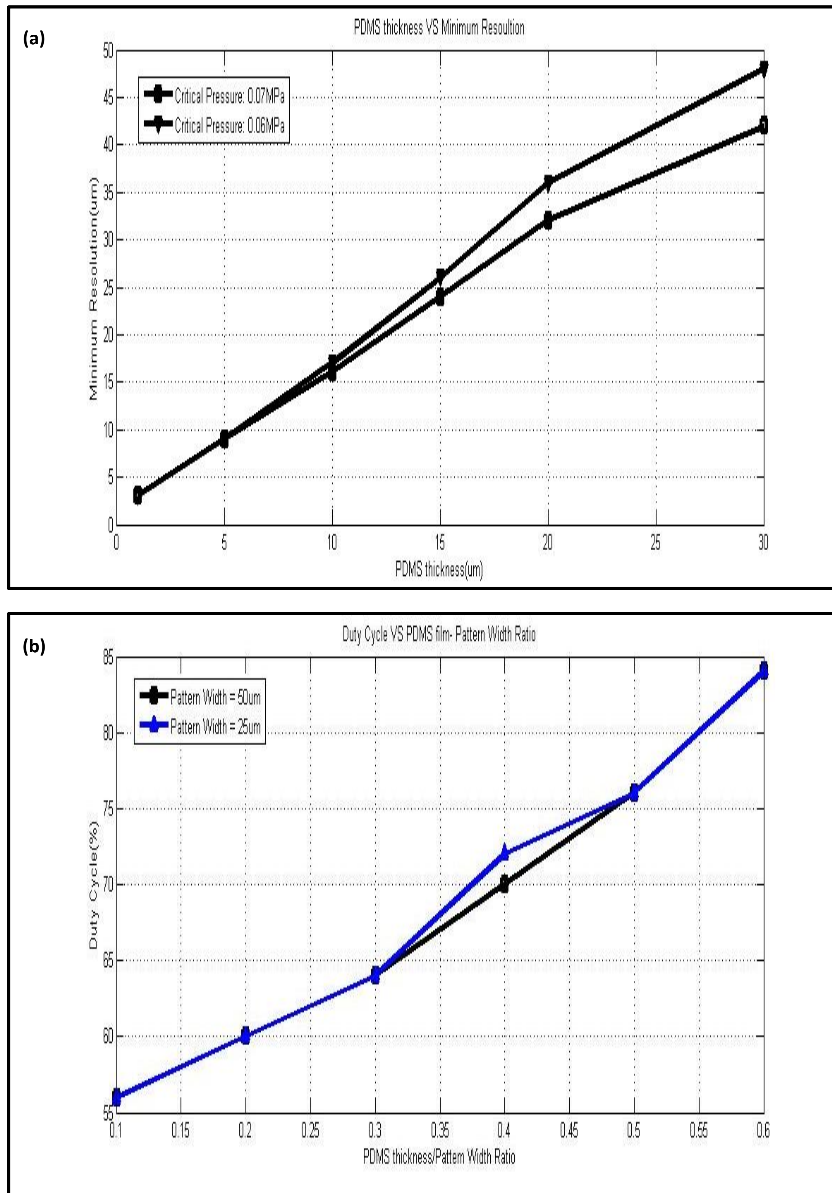

Figure 22 Process analysis graphs. (a)PDMS film thickness VS Process minimum resolution graph. (b)Duty cycle VS PDMS film thickness – pattern width Ratio graph.

REFERENCES

1. Campbell, S.A., *Fabrication engineering at the micro and nanoscale*. 3rd ed. The Oxford series in electrical and computer engineering. 2008, New York: Oxford University Press. xiv, 647 p.
2. Hu, C., *Modern semiconductor devices for integrated circuits*. 2010, Upper Saddle River, N.J.: Prentice Hall. xv, 351 p.
3. Gu, X.Y., et al., *A New Materials-based Pitch Division Technique.* Journal of Photopolymer Science and Technology, 2009. **22**(6): p. 773-781.
4. Lim, C.-M., et al., *Positive and negative tone double patterning lithography for 50nm flash memory.* Proc. SPIE 6154, Optical Microlithography XIX, 2006: p. 615410.
5. ITRS. 2009; Available from: http://www.itrs.net/Links/2009ITRS/Home2009.htm.
6. Sivakumar, S., *EUV lithography: Prospects and challenges.* Design Automation Conference (ASP-DAC), 2011 16th Asia and South Pacific, 2011: p. 402.
7. Gwyn, C.W., et al., *Extreme ultraviolet lithography.* Journal of Vacuum Science & Technology B: Microelectronics and Nanometer Structures, 1998. **16**(6): p. 3142-3149.
8. Wu, B. and A. Kumar, *Extreme ultraviolet lithography: A review.* Journal of Vacuum Science & Technology B: Microelectronics and Nanometer Structures, 2007. **25**(6): p. 1743-1761.

9. Chou, S.Y., P.R. Krauss, and P.J. Renstrom, *Imprint of sub-25 nm vias and trenches in polymers.* Applied Physics Letters, 1995. **67**(21): p. 3114-3116.

10. Chou, S.Y., P.R. Krauss, and P.J. Renstrom, *Imprint lithography with 25-nanometer resolution.* Science, 1996. **272**(5258): p. 85-87.

11. Chou, S.Y., et al., *Sub-10 nm imprint lithography and applications.* Journal of Vacuum Science & Technology B, 1997. **15**(6): p. 2897-2904.

12. Guo, L.J., *Nanoimprint lithography: Methods and material requirements.* Advanced Materials, 2007. **19**(4): p. 495-513.

13. Ahn, S.H. and L.J. Guo, *Large-area roll-to-roll and roll-to-plate nanoimprint lithography: A step toward high-throughput application of continuous Nanoimprinting.* ACS Nano, 2009. **3**(8): p. 2304-2310.

14. Tan, H., A. Gilbertson, and S.Y. Chou, *Roller nanoimprint lithography.* Journal of Vacuum Science & Technology B, 1998. **16**(6): p. 3926-3928.

15. Chou, S.Y., C. Keimel, and J. Gu, *Ultrafast and direct imprint of nanostructures in silicon.* Nature, 2002. **417**(6891): p. 835-837.

16. Chen, C.H., et al., *IR laser-assisted micro/nano-imprinting.* Journal of Micromechanics and Microengineering, 2006. **16**(8): p. 1463-1467.

17. Lee, Y.C., et al., *Roller-based laser-assisted direct imprinting for large-area and continuous nano-fabrication.* Microelectronic Engineering, 2010. **87**(1): p. 35-40.

18. Forrest, S.R., *The path to ubiquitous and low-cost organic electronic appliances on plastic.* Nature, 2004. **428**(6986): p. 911-918.

19. Shimoda, T., et al., *Inkjet printing of light-emitting polymer displays.* MRS Bulletin, 2003. **28**(11): p. 821-827.

20. Burrows, P.E., et al., *Organic vapor phase deposition: a new method for the growth of organic thin films with large optical non-linearities.* Journal of Crystal Growth, 1995. **156**(1–2): p. 91-98.

21. Chen, L.C., P. Degenaar, and D.D.C. Bradley, *Polymer transfer printing: Application to layer coating, pattern definition, and diode dark current blocking.* Advanced Materials, 2008. **20**(9): p. 1679-+.

22. Thangawng, A.L., et al., *An ultra-thin PDMS membrane as a bio/micro-nano interface: fabrication and characterization.* Biomed Microdevices, 2007. **9**(4): p. 587-595.

23. *Adhesions of CYCLOTENE advanced electronics resin. The Dow Chemical Company*. 2012; Available from: http://www.dow.com/cyclotene/resource/prodlit.htm.

24. Lin, S.L., et al., *BCB-to-oxide bonding technology for 3D integration.* Microelectronics Reliability, 2012. **52**(2): p. 352-355.

25. Cook, S., A. Furube, and R. Katoh, *Analysis of the excited states of regioregular polythiophene P3HT.* Energy & Environmental Science, 2008. **1**(2): p. 294-299.

26. Lin, I.K., et al., *Viscoelastic Characterization and Modeling of Polymer Transducers for Biological Applications.* Microelectromechanical Systems, Journal of, 2009. **18**(5): p. 1087-1099.

27. Tooley, W.W., et al., *Thermal fracture of oxidized polydimethylsiloxane during soft lithography of nanopost arrays.* Journal of Micromechanics and Microengineering, 2011. **21**(5): p. 054013-054022.